Title
A Split-Abl Kinase for Direct Activation in Cells

Journal
Cell Chemical Biology, 24(10)

ISSN
2451-9456

Authors
Diaz, Juan E
Morgan, Charles W
Minogue, Catherine E
et al.

Publication Date
2017-10-01

DOI
10.1016/j.chembiol.2017.08.007

Peer reviewed

HHS Public Access

Author manuscript

Cell Chem Biol. Author manuscript; available in PMC 2018 October 19.

Published in final edited form as:

Cell Chem Biol. 2017 October 19; 24(10): 1250–1258.e4. doi:10.1016/j.chembiol.2017.08.007.

A Split-Abl Kinase for Direct Activation in Cells

Juan E. Diaz[*,1,7], **Charles W. Morgan**[*,1,8], **Catherine E. Minogue**[2,9], **Alexander S. Hebert**[3], **Joshua J. Coon**[2,3,4,5], and **James A. Wells**[1,6,‡]

[1]Department of Pharmaceutical Chemistry, University of California San Francisco, San Francisco, California, 94158 USA

[2]Departments of Chemistry, University of Wisconsin, Madison, Wisconsin, 53706 USA

[3]Genome Center of Wisconsin, Madison, Wisconsin, 53706 USA

[4]Department of Biomolecular Chemistry, University of Wisconsin, Madison, Wisconsin, 53706 USA

[5]Morgridge Institute for Research, Wisconsin, 53706 USA

[6]Department of Cellular & Molecular Pharmacology, University of California, San Francisco, California, 94158 US

Summary

To dissect the cellular roles of individual kinases, it is useful to design tools for their selective activation. We describe the engineering of a split-cAbl kinase(sKin-Abl) that is rapidly activated in cells with rapamycin and allows temporal, dose, and compartmentalization control. Our design strategy involves an empirical screen in mammalian cells and identification of split site in the N-lobe. This split site leads to complete loss of activity, that can be restored upon small molecule-induced dimerization in cells. Remarkably, the split site is transportable to the related Src Tyr kinase and the distantly related Ser/Thr kinase, AKT, suggesting broader applications to kinases. To quantify the fold-induction of phosphotyrosine(pTyr) modification, we employed quantitative proteomics, NeuCode-SILAC. We identified a number of known Abl substrates, including autophosphorylation sites and novel pTyr targets, 432 pTyr sites in total. We believe this split-kinase technology will be useful for direct activation of protein kinases in cells.

In Brief

‡Corresponding & Lead Author: Jim.Wells@ucsf.edu.
*These authors contributed equally
[7]Present Address: Xencor, Monrovia, CA 91016 USA
[8]Present Address: MRC Laboratory of Molecular Biology, Cambridge, CB2 0QH UK
[9]Present Address: Department of Chemistry, Hartwick College, Oneonta, NY 13820 USA

Author Contributions: Conceptualization, J.E.D and J.A.W; Investigation, J.E.D., C.W.M., A.S.H. and C.E.M, Formal Analysis C.W.M., J.E.D., A.S.H., and C.E.M, Writing – Original Draft, C.W.M, J.E.D, and J.A.W. Writing – Review & Editing C.W.M, J.J.C, and J.A.W. Funding Acquisition, J.E.D., J.J.C, and J.A.W., Supervision J.A.W and J.J.C

Diaz, J., and Morgan, C., et al. detail their engineering cABL kinase into a small molecule activatable variant that is rapidly and selectively activated in mammalian cells and proceed to utilize NeuCode SILAC quantitative phosphoproteomics to identify known substrates and expose known and novel downstream targets of cAbl activation.

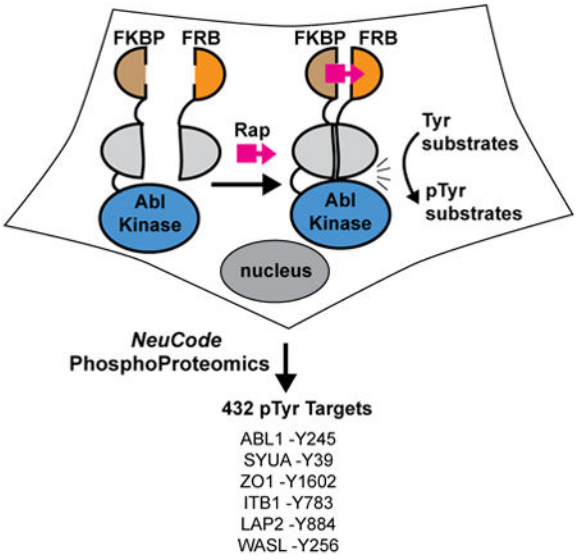

Keywords

Split-Protein Engineering; Protein Kinase; Selective Kinase Activation; Phosphoproteomics; NeuCode

Introduction

The human genome contains 518 protein kinases that control many intracellular signal transduction cascades(Neet and Hunter, 1996, Manning et al., 2002). Unregulated kinase activity leads to numerous diseases and has spawned research and development of targeted drug therapies(Greuber et al., 2013, Koleske, 2006, Sawyers, 2004, Cohen, 2002). Modern phosphoproteomics has identified nearly 300,000 phosphorylation sites in the human proteome, and at least one third of human proteins can be phosphorylated(Cohen, 2000, Olsen et al., 2006). Because phosphorylation and dephosphorylation events are dynamic and occur within the minutes time regime(Johnson et al., 2013, Sturani et al., 1988, Macdonald-Obermann et al., 2013), having a means to directly modulate a kinase in a cell is important to the field. Indeed, small molecule inhibitors can provide temporal and dose control, but they often have variable selectivity(Bain et al., 2003, Davies et al., 2000, Godl et al., 2003, Knight and Shokat, 2005). Allele-specific kinase inhibitors have improved our ability to selectively inhibit specific kinases, thus enabling us to more surgically interrogate the consequences of kinase inhibition. Others have designed photoactivable inhibitors of kinases by using inhibitory peptides fused to the LOV domain, which can provide single cell resolution and tight temporal inhibitory control(Yi et al., 2014).

All of these strategies above infer function through loss-of-function as opposed to gain-of-function. There has been significant progress in designing new small-molecule activated and light-activated kinases(Karginov et al., 2010, Gautier et al., 2011, Camacho-Soto et al., 2014a, Dagliyan et al., 2016, Zhou et al., 2017). We focused on a cAbl tyrosine kinase, whose direct activation in cells has not been achieved, and is disregulated in diseases caused by the Bcr-Abl oncogene. cAbl binds a range of cellular proteins, including kinases, phosphatases, cytoskeletal proteins, and transcription factors, among others(Brehme et al., 2009). Adding further complexity, cAbl has multiple subcellular locations, including the cytosol, nucleus, mitochondria, cell cortex, and endoplasmic reticulum(Hantschel and Superti-Furga, 2004). Unlike Src, Abl family members contain domains C-terminal to the SH3-SH2-kinase domain (KD) that include nuclear localization sequences (NLS), and nuclear export sequence (NES) and cytoskeleton binding domains. The cAbl kinase is believed to be activated in the cytosol in response to growth factor stimulation with subsequent migration to the nucleus(Hantschel and Superti-Furga, 2004). To develop a tool to begin to study these events we designed a small molecule activated split-cAbl kinase that is confined to the cytosol.

Here we describe a split kinase cAbl (sKin-Abl) that is brought together with rapamycin using conditional-induced dimerization (CID). We employed classic rapamycin-induced dimerization of FKBP and FRB (Spencer et al., 1993) fused to two protein fragments of Abl. Many fragmented enzymes and proteins have been based on CID and Protein fragment Completion Assay (PCA) (Michnick et al., 2007) for building biosensors, reporters, and inducible enzymes such as Horse radish peroxidase(Martell et al., 2016), TEV protease(Wehr et al., 2006, Gray et al., 2010), and Cas9 (Wright et al., 2015b, Zetsche et al., 2015, Nguyen et al., 2016, Wright et al., 2015a). Drawing inspiration by previous split protein engineering strategies, e.g., the dissection of the N and C-terminal lobes of the aminoglycoside kinase (Michnick et al., 2000), the sKin-Abl was designed using a step-wise structure-based approach (Figure 1A). Furthermore, we designed the sKin-Abl to be confined to the cytosol and rapidly activated only in the presence of rapamycin at concentrations that still allow the function of the endogenous rapamycin target, mTOR. To provide an unbiased proteomic analysis of the induced changes in the phosphotyrosine (pTyr) proteome, we employed NeuCode SILAC (Richards et al., 2013, Hebert et al., 2013a, Merrill et al., 2014a). We detected both known and novel pTyr events linked to sKin-Abl activation including Abl itself and proteins associated with cell migration. This approach provides a new tool for understanding the consequences for direct cellular activation of Abl and potentially other kinases as well.

Results

Design, Optimization, Characterization of split-Kinases

To guide our efforts in engineering the sKin-Abl we used three design principles common to other split-sensors and split-enzymes. First, for rapid induction the protein fragments need to be stable and easily expressed in cells. Second, the fragments must be inactive by themselves or when co-expressed. Finally, dimerization (in both constitutive and inducible dimerization modes) must rapidly rescue kinase activity. These design principles formed the

basis of our two-step procedure (Figure 1A). In step one, we produced nine fragmented Abl kinases and triaged them for those that were inactive when co-expressed in mammalian cells, but active when linked to constitutively active anti-parallel leucine zipper dimers(Ghosh et al., 2000). Employing the leucine zipper step facilitated the isolation of each stage of the design and testing process: the fragments are stably expressed and bringing them together reconstitutes activity. In the second step, we replaced the leucine zippers with the rapamycin-induced dimerization domains, FKBP and FRB, and tested each pair for rapamycin-dependent rescue of activity.

Before engineering the sKin-Abl, we designed a base construct that would localize cAbl to the cytosol so that we could identify the first wave of substrates there. We removed the N-terminal exon containing the myristate modification site, found in some Abl isoforms, and the C-terminal domains harboring the C-terminal NLS and cytoskeletal binding domains. Doing so produced a three-domain variant (3D-Abl) that included the SH3, SH2, and kinase domains (KD) of cABL1, residues 83-532. The structurally conserved KD comprises two well-defined lobes, the N-terminal lobe (N-lobe) and the C-terminal lobe (C-lobe), joined by a flexible hinge region. The smaller N-lobe consists of a five-stranded β-sheet and one α-helix, termed the αC helix. The larger C-lobe is primarily α-helical and contains the flexible activation loop, which mediates substrate binding (Figure 1B)(Schindler et al., 2000). We targeted both lobes to assess functional split sites (Figure 1C).

Activation of cAbl occurs through phosphorylation on Tyr245, either by an up-stream kinase or, once phosphorylated, by cAbl itself(Koleske, 2006). We aimed to disable endogenous cAbl activity using the drug imatinib without affecting the engineered variant. Thus, we introduced the T315I gatekeeper mutation to render the engineered variant resistant to the drug imatinib (Schindler et al., 2000). This construct provided a useful control for determining the contribution from the activated sKin-Abl that subsequently phosphorylates itself and other endogenous Abl family members. We found that the C-terminally FLAG-tagged version of 3D-Abl was well expressed by transient transfection in HEK293 cells (Figure 2A). The base construct (3D-Abl) was autophosphorylated (Figure 2B). Lastly, 3D-Abl induced extensive tyrosine phosphorylation (pTyr) in cells relative to an empty vector control or an inactive catalytic site variant, D382N(Figure 2C).

We next evaluated a dozen fragmented constructs from nine sites (Figure 1B) based on the principle that insertions in loops tend to be more permissive than in secondary structures. We first tested whether the respective epitope-tagged split fragments could be expressed separately and together (Figure S1 & Table S1). For each split that passed the expression test, we created a series of fusion proteins in which heterodimeric antiparallel leucine zippers were attached to the split site with a flexible 2x (Gly_4-Ser) linker in between. These fusion proteins were then tested for self and cellular pTyr production in both orientations (NZ/CZ and CZ/NZ) to optimize the construct (Zip-Abl variants). The split site at the β2-β3 junction (residues 282/283) met our criteria – it behaved well in expression studies, showed no activity as fragments, and hetero-dimerization mediated by the antiparallel leucine zippers rescued kinase activity (Figure 2B-D & Figure S2). We believe a major contributing factor to the success of this fragmented site comes from breaking the kinase within the P-loop (Reddy and Aggarwal, 2012)

Rapamycin-inducible Cellular Activation of sKin-Abl

Having identified a functional split site, we replaced the NC/CZ domains in the Zip-Abl variant with FRB/FKBP domains, respectively, to create what we call sKin-Abl. The fragments were tested for expression after transient transfection in HEK 293 cells and for dose-dependent activation by rapamycin. The sKin-Abl fragments expressed suitably when co-transfected in HEK 293T cells and showed rapamycin-induced pTyr production in a dose-dependent fashion upon addition of 1-10nM rapamycin (Figure 2D). We also tested for inhibition of the mTOR complex by rapamycin. Although this is of less of concern for short term experiments, significant inhibition of S6 kinase (p70-S6K) is not desirable long-term. At the levels of rapamycin we routinely use (10 nM) we observed only minor inhibition of mTOR kinase activity by monitoring phosphorylation of S6K (Figures S3). In addition, the exogenous expression of the CID domains acts to protect mTOR from rapamycin mediated inhibition.

For more extensive characterization of the sKin-Abl we produced stable cell lines in HeLa cells by integrating the sKin-Abl gene using Lenti-virus(Kumar et al., 2001, Morsut et al., 2016). We observed similar levels of expression of both fragments in HeLa cells and a substantial increase in pTyr levels following addition of 10nM rapamycin (Figure 2E). Because we designed sKin-Abl with a T315I mutation, it was possible to test the contribution of the endogenous imatinib-sensitive cAbl to the overall pTyr pattern in HeLa cells by adding imatinib. Pretreatment with imatinib resulted in little effect on global pTyr levels following sKin-Abl activation, as measured by pan-specific pTyr immunoblotting, suggesting the endogenous cAbl is not contributing significantly to the phosphorylation events. (Figure S4). To calibrate the timing of our proteomics sampling, we analyzed the time course of global pTyr labeling and showed it reaches saturation in about 20 minutes.

We next determined the cellular localization of the pTyr produced by sKin-Abl upon rapamycin-induction using immunofluorescence (Figure 3). Within a 20-minute treatment with rapamycin we observed a dramatic increase in pTyr staining throughout the cytosol. Staining in the nucleus was absent. This observation suggests that removal of the large C-terminal domains of Abl, containing three NLS sequences confines sKin-Abl pTyr activity predominately to the cytosol (Shaul, 2000).

Characterization of sKin-Abl Activation by Quantitative Phosphoproteomics

To evaluate the activity of sKin-Abl we performed quantitative phosphoproteomic experiments to characterize the cellular consequences triggered by selective sKin-Abl activation in HeLa cells. Our first aim was to identify pTyr-containing events that increased following sKin-Abl activation using a duplex neutron-encoded stable isotope labeling in amino acid cell culture (NeuCode SILAC) strategy (Figure 4A). The NeuCode SILAC approach utilizes heavy lysine isotopologues that differ in exact mass by 36–12 milliDaltons (mDa). Under standard resolving powers used in high-throughput proteomic experiments (< 60,000), the closely spaced *m/z* peaks are not distinguished and appear as a single *m/z* value. However, at higher-resolving powers (>100,000) these isotopologues can be resolved revealing the NeuCode doublet which affords quantitative comparisons between the two conditions. The benefit of this scheme is that quantitative information can be accessed at

strategic times in the data acquisition sequence using high resolution scans(Hebert et al., 2013a), while the spectral complexity known to hinder standard SILAC experiments is masked during normal data collection steps. NeuCode SILAC also retains the quantitative accuracy and dynamic range to assess fold induction, a hallmark of standard SILAC experiments.

The NeuCode SILAC experiments were conducted in three biological replicates to increase coverage and confidence. HeLa cells were cultured with lysine isotopologue 602 ($^{13}C_6{}^{15}N_2$). Rapamycin was then added to activate sKin-Abl or isotopologue 080 ($^{8}H_2$), which received the control (vehicle) treatment (Figure 4A). After 20 min induction with rapamycin, we identified and quantified a total of 432 different pTyr isoforms (Figure 4B & Table S2). More than 75% of these pTyr sites have previously been identified as Class I phosphosites, a measure of high confidence in phospho-group localization(Olsen et al., 2006). Among the most induced pTyr peptides were the previously reported pTyr sites in cAbl: Tyr 245, Tyr276 and Tyr412/439 (Figure 4C)(Hantschel and Superti-Furga, 2004). The strongest pTyr induction was seen at Tyr245 (20-fold), located in the SH2-kinase-domain linker, which is crucial for full activation of cAbl. In addition, we observed a greater than five-fold increase of pTyr in the activation loop at Tyr276 and Tyr412/439. As shown in Figure 4D, there is a 20-fold range in the fold induction of the 72 substrates common across the three biological replicates. We detected a number of additional known Abl substrates, such as WASL, HSP7C, CDK5, CRK, CAV1, ITGB1, and PTPN11(Colicelli, 2010, Simpson et al., 2015, Goss et al., 2006). We also observed novel pTyr substrates downstream of sKin-Abl activation that are known to form a complex involved in cell adhesion: TJP1 (*ZO1*) tight junction signaling and assembly, and LAP2 (*ERINB*) adaptor protein. We also observe 8488 pSer/pThr events in the Neucode dataset (Table S3). Thus, activation of sKin-Abl sparks a cascade of phosphorylations including secondary pSer/pThr events.

P-loop split site is general to Src and AKT1 kinases

To begin to explore the generality of the split site in cAbl to other kinases, we tested the portability of the split site in the structurally conserved Src tyrosine kinase and an evolutionary distant serine/threonine kinase, AKT1. A sKin-Src [84-287/288-536] variant split in the analogous P-loop site as sKin-Abl showed a rapamycin dose-dependent increase in total pTyr by Western blot (Figure S5A). The sKin-Src kinase could be activated with increasing concentrations of rapamycin (10 nM and saturating at 100 nM). We observed low levels of pTyr phosphorylation in the absence of rapamycin, which could reflect some constitutive activation of sKin-Src.

We also tested a Zip-AKT1 kinase fused to NZ/CZ leucine zippers and fragmented between residues 171/172. The Zip-AKT1 was assayed for phosphorylation at two key residues (Thr308 and Ser473) required for full activation of AKT1 (Figure S5B)(Vivanco and Sawyers, 2002). Activation of AKT1 occurs in two steps. First, the PH domain of AKT1 recruits the kinase to the membrane where PDK1 kinase phosphorylates Thr308. Second, for full AKT1 activity to be achieved, AKT1 must then interact and be phosphorylated by mTOR at Ser473. In the Zip-AKT1 variant [1-171/172-480], the PH domain is located on fragment 1, thus requiring both split halves to dimerize for phosphorylation of residues T308

and S473 to occur. Phosphorylation on these residues only occurs when both fragments are co-expressed in cells (Figure S5B). Co-expression of fragments fused to only one of the domains of the dimer pair (either FRB or CZ) does not lead to phosphorylation and activation of AKT1. The success and generality of the P-loop split sites on various sKin variants suggests the approach may be applicable to a large number of kinases that share the highly conserved kinase fold.

Discussion

The ability to dissect the function of individual protein kinases in driving signaling pathways at spatial and temporal levels is critically important to understanding of their roles in biology and disease. The direct activation of the EGF receptor tyrosine kinase with its natural ligand, EGF, provides a natural opportunity for determining the kinetics of the immediate phosphoproteome through direct kinase activation(Brasher and Van Etten, 2000, Johnson et al., 2013). However, for more distal kinases it is not possible to directly activate them without protein engineering. The sKin-Abl provides a useful tool for direct ignition of the kinase in the cytosol, allowing observation of phosphorylation-dependent consequences. We believe combining split-kinase engineering with quantitative multiplexed proteomics provides broad network-level probe of cytosolic Abl.

Given the importance of directly activating distal kinases, a surge of research has been directed to engineer them. For example, the Chin group elegantly produced a photo-caged MEK-activatable variant utilizing expanded genetic code techniques and most recently the Lin group published results of their photo-reversible MEK variant relying on active site steric occlusion (Gautier et al., 2011, Zhou et al., 2017). The Karginov and Hahn groups designed a destabilized FKBP (iFKBP) that was strategically inserted into focal adhesion kinase (FAK) between residues 442-448 in a loop between b2 and b3 in the N-lobe(Karginov et al., 2010). More recently they have expanded their engineering approach to Src family members(Chu et al., 2014). In their first example, iFKBP destabilized FAK and suppressed activity in the absence of rapamycin, but could be activated about 10-fold by stabilizing the FAK-iFKBP upon addition of rapamycin. The activated FAK-iFKBP stimulated appropriate autophosphorylation and phosphorylation of known candidate targets Src and paxcillin in cells by Western blotting. The destabilized iFKBP required high concentrations of rapamycin (200nM) for maximal stimulation, well above the IC_{50} (~20nM) for inhibition of S6 kinase(Ma and Blenis, 2009). Alternatively, Hahn and colleagues have inserted a LOV2 domain into Src for a photo-inhibitable kinase(Dagliyan et al., 2016).

Recently, the Ghosh group showed that poorly conserved loops in the N-lobe of Lyn kinase can tolerate large engineered loop insertions and are thus maybe amenable to split-protein engineering(Camacho-Soto et al., 2014a). Sequence alignments of tyrosine kinase family members identified both loops between β2/β3 and β4/β5 site in Lyn as being poorly conserved(Camacho-Soto et al., 2014b). Characterization by *in vitro* transcription and translation showed about a 10-fold induction of kinase activity when incubated with 200nM rapamycin. Cellular experiments were limited to split kinase expression and kinase activity assays against a Lyn peptide in lysate pulldown experiments. The Ghosh, Karginov and

Hahn groups have demonstrated generality to several other kinases, but not cAbl, and neither study reported cellular proteomics data to identify the resulting phosphoproteomes. Together these and our studies suggest a number of possible approaches to directly activate single protein kinases and thus further enable the broader kinase community.

Our approach to sKin-Abl involved a two-step approach similar to Ghosh and co-workers. However, in our first step we deliberately expressed fragments as antiparallel hetero-oligomerization leucine zippers to more closely mimic the assembly of separate polypeptides to be expressed in the final split-kinase. The constructs were expressed directly in mammalian cells because our end goal was to monitor cellular function. The location of the successful fragments surprised us because the small N-terminal β-hairpin fragment in the kinase domain is not an isolated folding domain. Nevertheless, this site appears general to other kinases, such as the related pTyr kinase, Src, or a distantly related pSer/pThr kinase, AKT. Additional engineering is likely required to tune and optimize the rapamycin responsiveness in sKin variants of Src and AKT. Others have similarly observed highly asymmetric fragments in single domain proteins that are capable of protein complementation when co-expressed, such as for GFP, RNase, and Ubiquitin(Hu et al., 2002, Richards, 1958, Johnsson and Varshavsky, 1994). Our work relied on an unbiased empirical screening approach to placing the CID domains in loops because it is challenging to rationally select specific functional fragmentation sites. Encouragingly, our work, along with the studies noted above, reveal several places in the N-lobe that will accept the CID domains and retain kinase function for a number of kinase family members.

The initiation of pTyr phosphorylation in sKin-Abl occurs within minutes, suggesting rapid assembly of the fragments. However, we cannot be sure activation for the natural cAbl is not faster since sKin-Abl needs to assemble from existing fragments. We engineered the gatekeeper T315I mutation into sKin-Abl to make it resistant to the pharmacological inhibition by imatinib. Addition of imatinib did not change the pTyr profiles significantly (Figure S4). Thus, the endogenous imatinib-sensitive pool is either far less active, or, like the engineered sKin-Abl, is largely confined to the cytosol. Distinguishing among these possibilities will require further research.

The highly quantitative aspect of NeuCode SILAC allowed precise estimates of fold-induction of pTyr event at an end point (20 min) where most of the pTyr targets had reached steady state. Among the most induced pTyr sites were the three known Tyr autophosphorylation sites of cAbl itself (Y245, Y276 and Y412/439). We did not detect pTyr204 in the SH2 domain or pTyr 488 in the C-lobe, which have been previously reported (reviewed in (Hantschel and Superti-Furga, 2004). The function of these two sites is unknown, but there has been speculation that they form an interface with the last exon of cAbl, which is missing in our sKin-Abl construct. The prominent pTyr245 that we observe is considered to be required for full activation of cAbl (Brasher and Van Etten, 2000). Although the sKin-Abl is primarily responsible for initiating the observed pTyr events, we cannot rule out another intermediary tyrosine-specific kinase(s) contributing to the observed pTyr profiles; they may be undetected or initiated by one of the other phosphoproteins. Moreover, it is possible that the sKin-Abl engineering has altered its capacity and specificity

for interacting with other proteins and substrates, further experiments are needed to assess this possibility.

Beyond the known autophosphorylation events, we detected a number of other known Abl substrates in our sKin-Abl dataset, such as WASL, CRK, CDK1, PTN11, SRC8, and many more (see Table S3). One of the most interesting sets of substrates concerns the tight junction complex involved in cell adhesion. The Tight Junction Protein (TJP)-ZO1 (Y1602, 3 fold-change) was identified and quantified in the NeuCode (Table S2). The TJP-ZO family of proteins serve as adaptors in epithelial tight junction through both PDZ and SH3 domains(Matter and Balda, 2003). cAbl activity has previously been implicated in playing a role in viral entry at tight junctions by Rac-mediated actin rearrangement. Our data supports this general hypothesis and further suggests a novel mechanism of action through phosphorylation of tight junction proteins(Coyne and Bergelson, 2006, Woodring et al., 2003). Overall, the dataset we provide identifies useful candidate substrates worthy of much more detailed investigation.

Our design and microscopy data support the conclusion that sKin-Abl is primarily active in the cytosol, with the large bulk of pTyr substrates showing a high level of phosphorylation are retained there. Our data suggest that the pTyr proteins we identified have a significant footprint in the cytosol. Future experiments are needed to characterize individual substrate's sub-cellular localization dependence on Abl mediated phosphorylation and provide corroborating evidence for the sub-cellular localization of sKin-Abl. Although we have only evaluated the cytosolic form of sKin-Abl, sKins can be made to the longer forms of cAbl, p185 and p210, as well as Bcr-Abl. This is a worthy experiment since the Hantschel and Superti-Furga groups have shown these forms have different interacting partners using affinity mass spectrometry(Brehme et al., 2009, Rix et al., 2007). Moreover, Bcr-Abl fusions show additional sites of autophosphorylation, such as Y272 and Y488(Hantschel and Superti-Furga, 2004). The dose dependent activity of sKin-Abl over the range of 1-10nM rapamycin would also allow one to investigate the immediate phosphoproteomes following varying levels of pathway stimulation by sKin-Abl. We believe sKin designs, coupled with proteomic and cellular characterization, will help us understand the role of specific temporal activation of kinases and the larger signaling networks they control.

Significance

Conditional enzyme activation strategies, such as split Kinases (sKins), are enable studying signaling with unprecedented temporal control and selectivity. Traditionally, kinases and their cellular functions are interrogated by genetic loss or inhibition studies; however diseases stemming from dysregulated kinase function predominately result from activation and or loss of feedback regulation. Thus, we engineered a split protein kinase that relies on chemical-induced dimerization using rapamycin for rapid cellular activation of the tyrosine kinase, cAbl confined to the cytosol. Furthermore, we employed quantitative NeuCode phosphoproteomics to identify downstream targets of cAbl. The sKins approach appears general to other kinases and provides an important platform for detailed characterization of the temporal and spatial characteristics of phospho-protein signaling.

STAR Methods

Contact for Reagents and Resource Sharing

Further information and requests for resources and reagents should be directed to and will be fulfilled by the Lead Contact, James Wells (Jim.Wells@ucsf.edu). sKin-Abl plasmids will be made available on Addgene following publication.

Experimental Model and Subject Details

Cell Lines—Human embryonic kidney 293T and HeLa cell lines were cultured at 37 °C, 5% CO_2 in DMEM-high glucose (Thermo Scientific) supplemented with 10% (v/v) fetal bovine serum (FBS, Gibco), 4 mM/L L-Glutamine, sodium pyruvate, non-essential amino acids, and penicillin/streptomycin (Pen/Strep, 100 U/mL). The 293-GPG retrovirus packaging cell line (Ory et al., 1996) was cultured in DMEM high glucose, 10% FBS, L-Glutamine, Pen/Strep, 1 μg/mL tetracycline, 2 μg/mL puromycin, 300μg/mL G418 at 37 °C, 5% CO_2.

Methods Details

Cloning Strategy and Construction of split-Kinase

Vector Construction: We constructed a series of mammalian transient expression vectors along with compatible retroviral producing vectors for generating stable cell lines. N-terminal Abl (res 83-263), Src (res 84-287), and AKT (res 1-171) fragments were PCR amplified and cloned with NotI and BamHI into a modified pcDNA3.1 backbone containing a C-terminal flexible 12-mer GlySer linker (GSGGGGSGGGGS) followed by the NZ-FLAG tagged antiparallel hetero-oligomerization leucine zipper helix (Ghosh et al., 2000). C-terminal Abl (res 264-532), Src (res 288-536), and AKT (res 172-480) fragments were cloned into a pcDNA3.1 Myc-CZ-GS_{12}-backbone using BamHI and EcoRI flanking sites. A second set of pcDNA3.1 vectors were constructed where the NZ and CZ fusions were replaced with-GS_{12}-FRB-Myc and FLAG-FKBP-GS_{12}-, respectively. The FRB and FKBP cloning cassettes were also introduced into pQCXI retroviral backbones (Clontech) containing either a Hygromycin (FRB vector) or Puromycin (FKBP vector) resistance gene for selecting stable integrant following viral transduction of target cell lines.

Transient Transfections

HEK293T cells (400,000) were seeded into a 6-well tissue culture plate and grown overnight at 37 °C, 5% CO_2 in DMEM-high glucose (Thermo Scientific) supplemented with 10% (v/v) fetal bovine serum (FBS, Gibco), 4 mM/L L-Glutamine, sodium pyruvate, non-essential amino acids, and penicillin/streptomycin (Pen/Strep 100 U/mL). The following day, all wells were washed with PBS and replaced with 2 mL of pre-warmed Opti-MEM-I (#31985-070, Life Technologies). Cells were transfected with Lipofectamine 2000 (Life Technologies) using a total of 4 μg of DNA per well (2 μg each of sKIN fragment [1] and [2] plasmids) according to the manufactures protocol. Six hours post-transfection, the medium was replaced with DMEM supplemented with 10% FBS and Pen/Strep before incubating at 37 °C, 5% CO_2 for 48 hours.

Western Blot

Cells were trypsinized, centrifuged at 300 rpm, washed once with ice-cold PBS and then lysed for 10 min on ice with M-PER reagent (ThermoFisher) supplemented with Sigma protease and phosphatase inhibitor cocktail mixtures. The crude lysate wad centrifuged at 14,000 rpm for 10 minutes at 4 °C. Clarified lys ates were flash frozen until further analysis by SDS-PAGE and immunoblotting. Protein loading was normalized by a standard BCA assay (Thermo Fisher). Proteins were separated on a 4-12% Tris-Glycine gel (BioRad) and transferred to a PVDF membrane. Membranes were blocked in 5% nonfat milk in PBS + 0.1% Tween-20 (PBST) for 30 minutes. The blocked PDVF membranes were washed three times in PBST before incubation with primary antibody (1:1000) in 5% nonfat milk-PBST for one hour at room temperature. PDVF membranes were washed three times in PBST before a final incubation of 30 minutes with secondary antibody (1:5000) in 5% nonfat milk-PBST. Blots were developed with ECL substrate and imaged using an Alpha Innotech FlourChem SP imaging system.

Retrovirus transduction

Virus production was performed by seeding 0.4×10^6 293-GPG cells per antigen in a 6-well plate 24h prior to transfection. On the day of transfection, the medium was replaced with Opti-MEM (Gibco) before cells were transfected with 4 μg pQCXIP-Abl [1] retroviral vector using Lipofectamine 2000 (Life Technologies) according to the manufacturer's protocol. Six hours post-transfection, the medium was replaced with DMEM supplemented with 10% FBS and Pen/Strep before incubating at 37 °C, 5% CO_2. Viral supernatants were harvested at 48 and 72h post-transfection, filtered (0.45 μm Millex HV, Millipore) and applied to 0.4×10^6 target HeLa cells in a 6-well plate and incubated overnight at 37 °C, 5% CO_2. Following the second viral transduction and overnight incubation, target cells were removed with 0.05% Trypsin/EDTA, transferred to 15 cm^2 dishes and grown in DMEM, 10% FBS, Pen/Strep for 48h prior to selection in Puromycin (1 μg/mL) containing medium. Selection medium was replaced once per week with fresh Puromycin-DMEM media until drug resistant foci (colonies) appeared. Stably integrated cells were expanded and analyzed for expression of sKin fragment by immunoblot before frozen stocks were made and stored in LN_2. The newly made HeLa-Abl [1] cell line was used as the target cell line for a second round of viral transduction using pQCXIH-Abl[2] retrovirus as described above. Dual expression of both Abl sKIN fragments was verified by immunoblot before frozen stocks were made and stored in vapor phase of liquid N_2.

Antibodies and reagents

Anti-FLAG M2 (#F1804) and anti-FLAG M2-HRP (#A8592) were purchased from Sigma-Aldrich and anti-Src antibody (#MA5-15120) was from Thermo Scientific. p-Src (Y416) (#2113), p-Abl (Y412) (#2865), p-Tyr-100 (#9411), p-Tyr-1000 (#8954), anti-GAPDH (#14C10), Myc Tag (mouse #2276 and rabbit #71D10), p-AKT (T308) (#13038), p-AKT (S473) (#4060), p70 S6 kinase (#9202), and phospho-p70 S6K (T389) (#9234) primary antibodies were purchased from Cell Signaling Technologies (CST). Secondary antibodies Goat anti-Mouse-HRP (#31430) and Goat anti-Rabbit-HRP (#31460) were from Thermo Scientific. Alexa Fluor 488 anti-mouse (#A11029) and Alexa Fluor 647 anti-rabbit

(#A21245) were from Life Technologies. All primary antibodies were used at a 1:1000 dilution and secondaries at 1:5000. Protease inhibitor cocktail (#P8340), Phosphatase inhibitor cocktail 2 (#P0044) and 3 (#P5726) were purchased from Sigma-Aldrich. NeuCode labeling reagents L-Lysine:2HCl (3,3,4,4,5,5,6,6-D8, 98%) (#DLM-2641-0) and L-Lysine: 2HCl (13C6, 99%, 15N2, 99%) (#CNLM-291-H-0.25) were from Cambridge Isotopes. Rapamycin was from Cayman Chemical and M-PER extraction reagent (#78501) was from Thermo Scientific. All restriction enzymes and DNA polymerases were purchased from NEB (Ipswich, MA). Oligonucleotides and gBlocks Gene Fragments were purchased from IDT and all constructs were verified by DNA sequencing (Quintara Biosciences).

Immunofluorescence

Split-Abl engineered Hela cells (100,000/well) were plated and grown to confluency on acid-washed glass coverslips (Fisher) for 24 hours. The following day, cells were treated for one hour with 10 nM Rapamycin or DMSO in complete DMEM media. Cells were fixed and permeabilized with 4% PFA in PBS for 15 minutes. Coverslips were washed with PBS + 0.1% Triton X-100 (PBS-TX) and then incubated with mouse anti-phospho-Tyr-100 (CST, 1:200) diluted in PBS-TX + 10% dialyzed FBS (Thermo Scientific) for 30 minutes at 37 °C. Coverslips were washed once with PBS for five minutes, washed once with PBS-TX for five minutes, then incubated with 1:100 Alexa Fluor 488 anti-mouse, DAPI 33342 for 30 minutes at 37 °C. Coverslips were mounted using SlowFade Gold (Molecular Probes) and visualized on a Ziess Axioobserver microscope.

Proteomic NeuCode labeling of sKin-Abl HeLa cells

sKin-Abl cells were passaged three times in DMEM lysine and arginine dropout medium (#89985, Thermo Scientific) supplemented with 10% dialyzed FBS (#88440, Thermo Scientific), pen/strep, 100 mg/L unlabeled L-arginine and 100 mg/L of either heavy [$^{13}C_6$, $^{15}N_2$] or light [D8] L-lysine (Cambridge Isotopes) for five passages, then transferred into 15 cm^2 tissue culture dishes for a final sixth passage in labeled media. At 90% confluency, cells were washed with PBS and fresh [$^{13}C_6$, $^{15}N_2$] L-lysine + DMSO (1:1000) or [D8] L-lysine + 10 nM Rapamycin (1:1000 of 10 μM stock) was added to cells for 20 min at 37 °C, 5% CO_2. Following rapamycin treatment, cells were washed with PBS, dissociated with Versene and transferred into 15 mL centrifuge tubes. Cells (~1 ×10^7 cells per condition) were centrifuged for five minutes at 300 rpm, the cell pellets flash frozen and stored at -80 °C until pro cessing.

Cells were resuspended and vortexed in 1 mL of lysis buffer (8 M Urea, 40 mM Tris, pH 8, 30 mM NaCl, 1 mM $CaCl_2$, 4 tabs of phosStop phosphatase inhibitor (Roche Diagnostics, Indianapolis, IN), 2 tabs of mini EDTA-free protease inhibitor (Roche Diagnostics, Indianapolis, IN), and 2 uL of benzonase. Protein content was evaluated using a BCA assay (Thermo Fisher Scientific). Proteins were reduced with 5 mM dithiothreitol (DTT) at 58°C for 45 minutes and alk ylated with 15 mM iodacetamaide at ambient temperature in the dark for 45 minutes. Alkylation was quenched by adding an additional 5 mM DTT at ambient temperature for 15 minutes. Proteins were digested with 50 ug of LysC (Wako Chemicals, Richmon, VA) for 17 hours, then an additional 25 ug of LysC was added for an additional 2 hours. Then the digest was quenched by bringing the pH to less than 2 with 10% TFA.

Samples were then immediately desalted using C18 solid-phase extraction columns (SepPak, Waters, Milford, MA). Desalted peptides were frozen until fractionation and enrichment.

Fractionation and enrichment

Peptides were fractionated by strong cation exchange (SCX) using a polysulfoethylaspartamide column (9.4×200mm; PolyLC) on a Surveyor LC quaternary pump (Thermo Scientific). Samples were resuspended in buffer A and injected onto the column. The gradient used for separation was 100% buffer A from 0-2 min, 0-15% buffer from 2-5 min, and 15-100% buffer B from 5-35 min. Buffer B was held at 100% for 10 minutes and then the column was washed extensively with buffer C and water prior to recalibration. Flow rate was held at 3.0 mL/min throughout the separation. Buffer compositions were as follows: buffer A [5mM KH_2PO_4, 30% acetonitrile (pH 2.65)], buffer B [5mM KH_2PO_4, 350mM KCl, 30% acetonitrile (pH 2.65)] buffer C [50mM KH_2PO_4, 500mM KCl (pH 7.5)]. Twelve fractions were collected over the first 50-minute elution period and were immediately frozen, lyophilized, and desalted.

Phosphopeptides were enriched using immobilized metal affinity chromatography (IMAC) with magnetic beads (Qiagen, Valencia, CA). After equilibration with water, the magnetic beads were incubated with 40mM EDTA (pH 8.0) for 1 hour while shaking. Next, the beads were washed four times with water and incubated with 30mM FeCl3 for 1 hour while shaking. Beads were then washed four times with 80% acetonitrile/0.15% TFA. Each of the SCX fractions were re-suspended in 80% acetonitrile/0.15% TFA and incubated with the magnetic beads for 45 minutes, with shaking. Unbound peptides were collected for protein analysis. Bound peptides were washed three times with 80% acetonitrile/0.15% TFA and eluted with 50% acetonitrile, 0.7% NH_4OH. Eluted peptides were immediately acidified with 4% formic acid, frozen, and lyophilized. Each phosphopeptide fraction was re-suspended in 35 μL 0.2% FA for LC-MS/MS analysis.

LC-MS/MS Analysis

NeuCode experiments were performed using a NanoAcquity UPLC system (Waters, Milford, MA) coupled to an Orbitrap Fusion (Q-OT-qlT) mass spectrometer (Thermo Fisher Scientific, San Jose, CA). Both LC systems used reverse-phased columns made in-house by packing a fused silica capillary (75μm i.d., 360 μm o.d, with a laser-pulled electrospray tip) with 1.7μm diameter, 130 Å pore size Bridged Ethylene Hybrid C18 particles (Waters) to a final length of 30cm. The columns were heated to 60°C for all experiments and peptides were eluted over a 70 minute gradient with mobile phase A (0.2% formic acid/5% DMSO) and mobile phase B (acetonitrile/0.2% formic acid). Precursor peptide cations were generated from the eluent through the utilization of a nanoESI source. Phospho-enriched fractions were each analyzed in duplicate for proteomic experiments.

Mass spectrometry instrument methods for NeuCode experiments consisted of precursor (MS1) survey scans at 240,000 resolution that were used to guide subsequent data-dependent MS/MS scans in top-speed mode. The ion accumulation values were set to 5E5 for the MS1 scans and 1E4 for the MS/MS scans.

Fragmentation for the MS/MS scans was HCD at 30% collision energy and analyzed in the ion trap. The maximum injection time was 75 ms for the MS1 and 100 ms for the MS/MS scans.

Quantification and Statistical Analysis

Data Analysis—NeuCode experiments were analyzed using Proteome Discoverer (Thermo Fisher Scientific, San Jose, CA). Proteome Discoverer was used for all data analysis except for quantitation which was down by in house NeuCode quantitation software, NeuQuant(Baughman et al., 2016, Merrill et al., 2014b, Hebert et al., 2013b). Searches were conducted using the SEQUEST search alogorithm with a 150 ppm precursor mass tolerance. The product mass tolerance was 0.35 Da and a maximum of three missed tryptic cleavages were allowed. Fixed modifications were carbamidomethylation of cysteine residues and NeuCode heavy lysine (+8.032 Da). Variable modifications were oxidation of methionine and then for phosphopeptide samples phosphorylation of threonine, serine, and tyrosine were also added. A false discovery rate of 1% was used at the peptide and protein level.

After database searching, the FDR-filtered list of peptide spectral matches was first used to calculate the systematic precursor mass error associated with the data set. After the adjustment of precursor masses for this error, every high-resolution MS1 scan within ±30 s of all PSMs identifying a unique peptide sequence was inspected. A quantitative pair was created for each labeled peptide precursors found within the specified tolerance (±5 p.p.m.) and exhibiting signal-to-noise greater than 3. The signal-to-noise values for each channel were summed across the peptide's elution profile to compensate for chromatographic shifts between isotopologues. Peaks below the noise level contributed a noise-based intensity to the appropriate missing channel. To eliminate the noise-capped peaks on the sides of a peptide's elution profile compressing the quantitative ratio toward 1:1, we discarded peaks with intensities below 1/(2e) times the maximum intensity (e refers to the mathematical constant). This peak filtering threshold is approximately the 1.75 s.d. of the standard normal distribution (the assumed shape of a peptide's elution profile); the distribution area covered by ± 1.75 s.d. is >90%. Peptides were required to have a minimum of three ratio-providing pairs (i.e., quantified across at least three MS1 scans) to be eligible for quantification.

Phosphopeptide localization was performed using PhosphoRS integrated with COMPASS(Taus et al., 2011). Unique protein groups were log2 transformed and then mean normalized within each NeuCode experiment before calculating ratios and p values. P-values were calculated using a two sample heteroscedastic t-test to compare each of the time points to the 0 minute time point. Significance was defined as a p-value of less than 0.05.

Supplementary Material

Refer to Web version on PubMed Central for supplementary material.

Acknowledgments

The authors would like to thank Drs. Jason Porter, JT Koerber, Zachary Hill, Julia Seaman, Ashley Smart, and Samantha Zeitlin for their helpful discussions and insight during research and analysis. We would like to thank the

UCSF Laboratory for Cell Analysis and Nikon Imaging Center for use of their flow cytometers and fluorescent microscopes. We thank the laboratory of John Kuriyan (UC Berkeley) for the gifts of cAbl and cSrc expression plasmids. This work was supported by grants from the National Institutes of Health NIGMS 1R01GM097316-01 and NCI R01 CA191018-01 to JAW, 1F32GM089082-01 to JED, NIGMS P41 GM108538 to JJC. NIH NRSA Postdoctoral Fellowship to JED and a NSF Graduate Research Fellowship to CWM and NMR (DGE-1256259). CEM was supported by an NLM training grant to the Computation and Informatics in Biology and Medicine Training Program (NLM T15LM007359)

References

Bain J, Mclauchlan H, Elliott M, Cohen P. The specificities of protein kinase inhibitors: an update. Biochem J. 2003; 371:199–204. [PubMed: 12534346]

Baughman JM, Rose CM, Kolumam G, Webster JD, Wilkerson EM, Merrill AE, Rhoads TW, Noubade R, Katavolos P, Lesch J, et al. NeuCode Proteomics Reveals Bap1 Regulation of Metabolism. Cell Rep. 2016; 16:583–95. [PubMed: 27373151]

Brasher BB, Van Etten RA. c-Abl Has High Intrinsic Tyrosine Kinase Activity That Is Stimulated by Mutation of the Src Homology 3 Domain and by Autophosphorylation at Two Distinct Regulatory Tyrosines. Journal of Biological Chemistry. 2000; 275:35631–35637. [PubMed: 10964922]

Brehme M, Hantschel O, Colinge J, Kaupe I, Planyavsky M, Kocher T, Mechtler K, Bennett KL, Superti-Furga G. Charting the molecular network of the drug target Bcr-Abl. Proc Natl Acad Sci U S A. 2009; 106:7414–9. [PubMed: 19380743]

Camacho-Soto K, Castillo-Montoya J, Tye B, Ghosh I. Ligand-Gated Split-Kinases. Journal of the American Chemical Society. 2014a; 136:3995–4002. [PubMed: 24533431]

Camacho-Soto K, Castillo-Montoya J, Tye B, Ogunleye LO, Ghosh I. Small molecule gated split-tyrosine phosphatases and orthogonal split-tyrosine kinases. J Am Chem Soc. 2014b; 136:17078–86. [PubMed: 25409264]

Chu PH, Tsygankov D, Berginski ME, Dagliyan O, Gomez SM, Elston TC, Karginov AV, Hahn KM. Engineered kinase activation reveals unique morphodynamic phenotypes and associated trafficking for Src family isoforms. Proc Natl Acad Sci U S A. 2014; 111:12420–5. [PubMed: 25118278]

Cohen P. The regulation of protein function by multisite phosphorylation--a 25 year update. Trends Biochem Sci. 2000; 25:596–601. [PubMed: 11116185]

Cohen P. Protein kinases--the major drug targets of the twenty-first century? Nat Rev Drug Discov. 2002; 1:309–15. [PubMed: 12120282]

Colicelli J. ABL tyrosine kinases: evolution of function, regulation, and specificity. Sci Signal. 2010; 3:re6. [PubMed: 20841568]

Coyne CB, Bergelson JM. Virus-induced Abl and Fyn kinase signals permit coxsackievirus entry through epithelial tight junctions. Cell. 2006; 124:119–31. [PubMed: 16413486]

Dagliyan O, Tarnawski M, Chu PH, Shirvanyants D, Schlichting I, Dokholyan NV, Hahn KM. Engineering extrinsic disorder to control protein activity in living cells. Science. 2016; 354:1441–1444. [PubMed: 27980211]

Davies SP, Reddy H, Caivano M, Cohen P. Specificity and mechanism of action of some commonly used protein kinase inhibitors. Biochem J. 2000; 351:95–105. [PubMed: 10998351]

Gautier A, Deiters A, Chin JW. Light-activated kinases enable temporal dissection of signaling networks in living cells. J Am Chem Soc. 2011; 133:2124–7. [PubMed: 21271704]

Ghosh I, Hamilton AD, Regan L. Antiparallel leucine zipper-directed protein reassembly: applicaion to the green fluorescent protein. J Am Chem Soc. 2000; 122:5658–5659.

Godl K, Wissing J, Kurtenbach A, Habenberger P, Blencke S, Gutbrod H, Salassidis K, Stein-Gerlach M, Missio A, Cotten M, et al. An efficient proteomics method to identify the cellular targets of protein kinase inhibitors. Proc Natl Acad Sci U S A. 2003; 100:15434–9. [PubMed: 14668439]

Goss VL, Lee KA, Moritz A, Nardone J, Spek EJ, Macneill J, Rush J, Comb MJ, Polakiewicz RD. A common phosphotyrosine signature for the Bcr-Abl kinase. Blood. 2006; 107:4888–97. [PubMed: 16497976]

Gray DC, Mahrus S, Wells JA. Activation of specific apoptotic caspases with an engineered small-molecule-activated protease. Cell. 2010; 142:637–46. [PubMed: 20723762]

Greuber EK, Smith-Pearson P, Wang J, Pendergast AM. Role of ABL family kinases in cancer: from leukaemia to solid tumours. Nat Rev Cancer. 2013; 13:559–71. [PubMed: 23842646]

Hantschel O, Superti-Furga G. Regulation of the c-Abl and Bcr-Abl tyrosine kinases. Nat Rev Mol Cell Biol. 2004; 5:33–44. [PubMed: 14708008]

Hebert AS, Merrill AE, Bailey DJ, Still AJ, Westphall MS, Strieter ER, Pagliarini DJ, Coon JJ. Neutron-encoded mass signatures for multiplexed proteome quantification. Nat Methods. 2013a; 10:332–4. [PubMed: 23435260]

Hebert AS, Merrill AE, Stefely JA, Bailey DJ, Wenger CD, Westphall MS, Pagliarini DJ, Coon JJ. Amine-reactive neutron-encoded labels for highly plexed proteomic quantitation. Mol Cell Proteomics. 2013b; 12:3360–9. [PubMed: 23882030]

Hu CD, Chinenov Y, Kerppola TK. Visualization of interactions among bZIP and Rel family proteins in living cells using bimolecular fluorescence complementation. Mol Cell. 2002; 9:789–98. [PubMed: 11983170]

Johnson H, Lescarbeau RS, Gutierrez JA, White FM. Phosphotyrosine Profiling of NSCLC Cells in Response to EGF and HGF Reveals Network Specific Mediators of Invasion. Journal of Proteome Research. 2013; 12:1856–1867. [PubMed: 23438512]

Johnsson N, Varshavsky A. Split ubiquitin as a sensor of protein interactions in vivo. Proc Natl Acad Sci U S A. 1994; 91:10340–4. [PubMed: 7937952]

Karginov AV, Ding F, Kota P, Dokholyan NV, Hahn KM. Engineered allosteric activation of kinases in living cells. Nat Biotechnol. 2010; 28:743–7. [PubMed: 20581846]

Knight ZA, Shokat KM. Features of selective kinase inhibitors. Chem Biol. 2005; 12:621–37. [PubMed: 15975507]

Koleske, AJ. Abl family kinases in development and disease. Georgetown, Tex New York: Landes Bioscience; Springer Science+Business Media; 2006.

Kumar M, Keller B, Makalou N, Sutton RE. Systematic determination of the packaging limit of lentiviral vectors. Hum Gene Ther. 2001; 12:1893–905. [PubMed: 11589831]

Ma XM, Blenis J. Molecular mechanisms of mTOR-mediated translational control. Nat Rev Mol Cell Biol. 2009; 10:307–18. [PubMed: 19339977]

Macdonald-Obermann JL, Adak S, Landgraf R, Piwnica-Worms D, Pike LJ. Dynamic analysis of the epidermal growth factor (EGF) receptor-ErbB2-ErbB3 protein network by luciferase fragment complementation imaging. J Biol Chem. 2013; 288:30773–84. [PubMed: 24014028]

Manning G, Whyte DB, Martinez R, Hunter T, Sudarsanam S. The protein kinase complement of the human genome. Science. 2002; 298:1912–34. [PubMed: 12471243]

Martell JD, Yamagata M, Deerinck TJ, Phan S, Kwa CG, Ellisman MH, Sanes JR, Ting AY. A split horseradish peroxidase for the detection of intercellular protein-protein interactions and sensitive visualization of synapses. Nat Biotech. 2016; 34:774–780.

Matter K, Balda MS. Signalling to and from tight junctions. Nat Rev Mol Cell Biol. 2003; 4:225–36. [PubMed: 12612641]

Merrill AE, Hebert AS, Macgilvray ME, Rose CM, Bailey DJ, Bradley JC, Wood WW, EL Masri M, Westphall MS, Gasch AP, et al. NeuCode labels for relative protein quantification. Mol Cell Proteomics. 2014a; 13:2503–12. [PubMed: 24938287]

Merrill AE, Hebert AS, Macgilvray ME, Rose CM, Bailey DJ, Bradley JC, Wood WW, EL Masri M, Westphall MS, Gasch AP, et al. NeuCode Labels for Relative Protein Quantification. Molecular & Cellular Proteomics. 2014b; 13:2503–2512. [PubMed: 24938287]

Michnick SW, Ear PH, Manderson EN, Remy I, Stefan E. Universal strategies in research and drug discovery based on protein-fragment complementation assays. Nat Rev Drug Discov. 2007; 6:569–82. [PubMed: 17599086]

Michnick SW, Remy I, Campbell-Valois FX, Vallee-Belisle A, Pelletier JN. Detection of protein-protein interactions by protein fragment complementation strategies. Methods Enzymol. 2000; 328:208–30. [PubMed: 11075347]

Morsut L, Roybal KT, Xiong X, Gordley RM, Coyle SM, Thomson M, Lim WA. Engineering Customized Cell Sensing and Response Behaviors Using Synthetic Notch Receptors. Cell. 2016; 164:780–91. [PubMed: 26830878]

Neet K, Hunter T. Vertebrate non-receptor protein-tyrosine kinase families. Genes Cells. 1996; 1:147–69. [PubMed: 9140060]

Nguyen DP, Miyaoka Y, Gilbert LA, Mayerl SJ, Lee BH, Weissman JS, Conklin BR, Wells JA. Ligand-binding domains of nuclear receptors facilitate tight control of split CRISPR activity. Nature Communications. 2016; 7:12009.

Olsen JV, Blagoev B, Gnad F, Macek B, Kumar C, Mortensen P, Mann M. Global, in vivo, and site-specific phosphorylation dynamics in signaling networks. Cell. 2006; 127:635–48. [PubMed: 17081983]

Ory DS, Neugeboren BA, Mulligan RC. A stable human-derived packaging cell line for production of high titer retrovirus/vesicular stomatitis virus G pseudotypes. Proceedings of the National Academy of Sciences of the United States of America. 1996; 93:11400–6. [PubMed: 8876147]

Reddy EP, Aggarwal AK. The ins and outs of bcr-abl inhibition. Genes Cancer. 2012; 3:447–54. [PubMed: 23226582]

Richards AL, Vincent CE, Guthals A, Rose CM, Westphall MS, Bandeira N, Coon JJ. Neutron-encoded signatures enable product ion annotation from tandem mass spectra. Mol Cell Proteomics. 2013; 12:3812–23. [PubMed: 24043425]

Richards FM. On the Enzymic Activity of Subtilisin-Modified Ribonuclease. Proceedings of the National Academy of Sciences of the United States of America. 1958; 44:162–166. [PubMed: 16590160]

Rix U, Hantschel O, Durnberger G, Remsing Rix LL, Planyavsky M, Fernbach NV, Kaupe I, Bennett KL, Valent P, Colinge J, et al. Chemical proteomic profiles of the BCR-ABL inhibitors imatinib, nilotinib, and dasatinib reveal novel kinase and nonkinase targets. Blood. 2007; 110:4055–63. [PubMed: 17720881]

Sawyers C. Targeted cancer therapy. Nature. 2004; 432:294–7. [PubMed: 15549090]

Schindler T, Bornmann W, Pellicena P, Miller WT, Clarkson B, Kuriyan J. Structural mechanism for STI-571 inhibition of abelson tyrosine kinase. Science. 2000; 289:1938–42. [PubMed: 10988075]

Shaul Y. c-Abl: activation and nuclear targets. Cell Death Differ. 2000; 7:10–6. [PubMed: 10713716]

Simpson MA, Bradley WD, Harburger D, Parsons M, Calderwood DA, Koleske AJ. Direct interactions with the integrin beta1 cytoplasmic tail activate the Abl2/Arg kinase. J Biol Chem. 2015; 290:8360–72. [PubMed: 25694433]

Spencer DM, Wandless TJ, Schreiber SL, Crabtree GR. Controlling signal transduction with synthetic ligands. Science. 1993; 262:1019. [PubMed: 7694365]

Sturani E, Zippel R, Toschi L, Morello L, Comoglio PM, Alberghina L. Kinetics and regulation of the tyrosine phosphorylation of epidermal growth factor receptor in intact A431 cells. Molecular and Cellular Biology. 1988; 8:1345–1351. [PubMed: 3367910]

Taus T, Kocher T, Pichler P, Paschke C, Schmidt A, Henrich C, Mechtler K. Universal and confident phosphorylation site localization using phosphoRS. J Proteome Res. 2011; 10:5354–62. [PubMed: 22073976]

Vivanco I, Sawyers CL. The phosphatidylinositol 3-Kinase AKT pathway in human cancer. Nat Rev Cancer. 2002; 2:489–501. [PubMed: 12094235]

Wehr MC, Laage R, Bolz U, Fischer TM, Grunewald S, Scheek S, Bach A, Nave KA, Rossner MJ. Monitoring regulated protein-protein interactions using split TEV. Nature methods. 2006; 3:985–93. [PubMed: 17072307]

Woodring PJ, Hunter T, Wang JY. Regulation of F-actin-dependent processes by the Abl family of tyrosine kinases. J Cell Sci. 2003; 116:2613–26. [PubMed: 12775773]

Wright AV, Sternberg SH, Taylor DW, Staahl BT, Bardales JA, Kornfeld JE, Doudna JA. Rational design of a split-Cas9 enzyme complex. Proc Natl Acad Sci U S A. 2015a; 112:2984–9. [PubMed: 25713377]

Wright AV, Sternberg SH, Taylor DW, Staahl BT, Bardales JA, Kornfeld JE, Doudna JA. Rational design of a split-Cas9 enzyme complex. Proceedings of the National Academy of Sciences of the United States of America. 2015b; 112:2984–2989. [PubMed: 25713377]

Yi JJ, Wang H, Vilela M, Danuser G, Hahn KM. Manipulation of Endogenous Kinase Activity in Living Cells Using Photoswitchable Inhibitory Peptides. ACS Synthetic Biology. 2014; 3:788–795. [PubMed: 24905630]

Zetsche B, Volz SE, Zhang F. A split-Cas9 architecture for inducible genome editing and transcription modulation. Nat Biotech. 2015; 33:139–142.

Zhou XX, Fan LZ, Li P, Shen K, Lin MZ. Optical control of cell signaling by single-chain photoswitchable kinases. Science. 2017; 355:836–842. [PubMed: 28232577]

Abbreviations

CID	Chemical Induced Dimerization
sKin	split-Kinase
pTyr	Phosphotyrosine

Highlights

- A split protein variant of cAbl kinase for rapid cellular activation
- Neucode-based phosphoproteomics characterizes selective activation
- Known and novel cAbl kinase downstream targets are identified and discussed

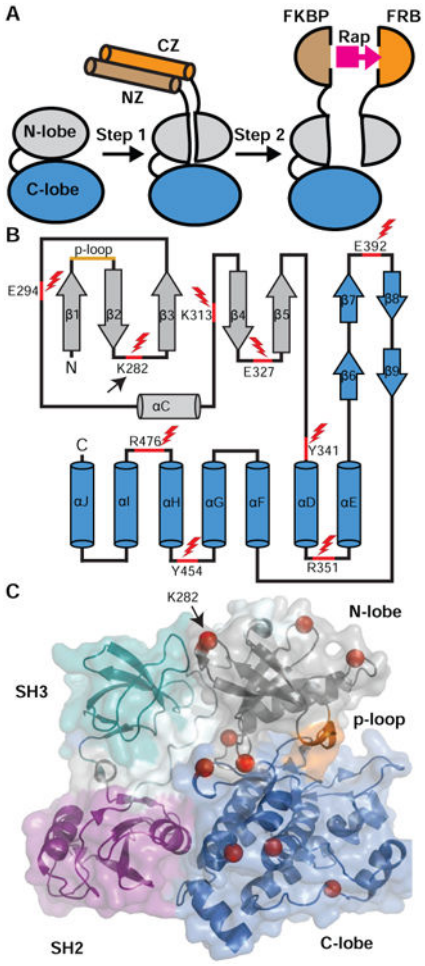

Figure 1. Split-Kinase strategy and fragmentation sites

(A) Schematic of our split-kinase (sKin) engineering strategy. The design strategy relies on a two-step process with biochemical and cellular testing at each step to ultimately achieve kinase activation only in the presence of a small molecule by conditional induced dimerization (CID). In the first step, the potential split-kinase variants are dissected in two fragments such that they each express in mammalian cells but do not exhibit activity either separately or when co-expressed. The two fragments are then forced to constitutively interact using dimerizing antiparallel hetero-oligomerization leucine zippers, NZ and CZ, (Zip-Abl variants). Successful fragments are shown to rescue kinase activity when co-expressed. The second step replaces the zippers with the well-known CID domains, FKBP and FRB. Successful constructs (sKins) initiate kinase activity in a cell upon addition of subtoxic doses of rapamycin (Rap).

(B) Topology diagram of typical kinase domain (KD). The N-lobe (light grey) is predominately composed of β-sheets while the C-lobe (blue) is mostly α-helical. Fragment sites between β-sheets and α-helices are highlighted by red lightning bolts in the N-Lobe and C-Lobe. The highly conserved p-loop is colored orange. N-terminal amino acid and residue number are located adjacent to fragment site. Numbering corresponds to cAbl isoform 1b. The most successful fragment site, K282 is indicated with an arrow. This site is

positioned at the top of the loop between the two highly evolutionarily conserved beta strands, β2 and β3. Diagram adapted from Camacho-Soto et al.

(C) Ribbon diagram of the three domain cAbl (3D-Abl) containing SH3-SH2-kinase domains with SH3 domain shown in teal, SH2 domain shown in purple, and kinase in grey (N-lobe) and blue (C-lobe). All tested fragmentation sites are depicted as spheres, they were chosen to intersect loop regions between β-sheets in the N-Lobe and α-helices in the C-lobe. Red spheres correspond to tested fragmentation sites. Adapted with PyMol from PDB: 2FO0.

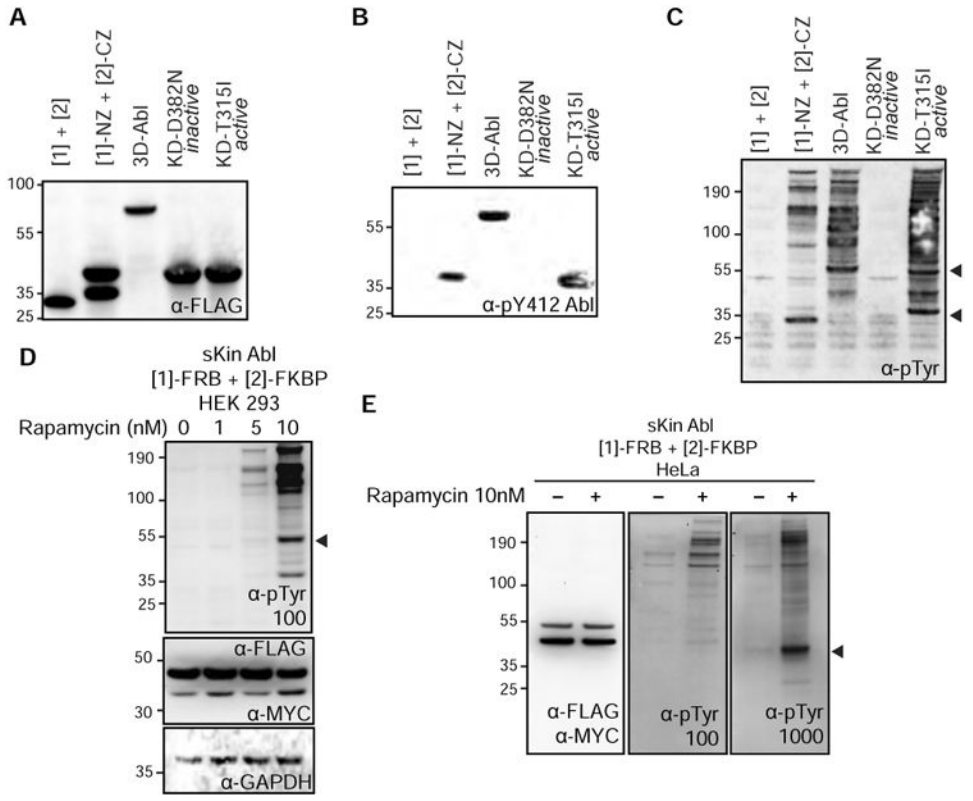

Figure 2. Design and testing of 3D-Abl constructs from Zip-Abl to sKin-Abl

(A) Transient expression of FLAG-tagged fragments of the Zip-Abl kinase in HEK293T cells shows the protein fragments are produced at comparable levels. Note that the molecular weight of [1] and [2] are not resolved on the gel so appear as one band when co-expressed.

(B) Autophosphorylation on the Abl activation loop Y412 for constructs in Panel A shows functional activity for 3D-Abl, Zip-Abl, but not non-dimerizing fragments. 3D-Abl fragments, [1] Abl 84-283 and [2] Abl 284-533, were inactive when co-expressed (left most lane) but when joined by leucine zippers (Zip-Abl) produced phosphorylation levels similar to the full length 3D-Abl or active T315I gate-keeper mutant of 3D-Abl.

(C) Immunoblot of total cellular pTyr for the constructs in Panel B shows global functional activity for 3D-Abl, Zip-Abl, but not non-dimerizing fragments. Extensive phosphotyrosine is observed upon co-expression of the N- and C-terminal leucine zipper fragments, as well as full length and KD containing the gate-keeper mutation but not for inactive KD or control lysate. Arrows indicates expected MW band corresponding to split-Abl fragment and activating pTyr (Y412) on pan-pTyr blots C-E.

(D) Global rapamycin-dependent pTyr phosphorylation (top panel) for skin-Abl fragments containing [1] linked to a MYC-tagged FRB and [2] linked to a FLAG-tagged FKBP and transiently co-expressed in HEK293 (middle panel). The split-Abl kinase could be activated with increasing concentrations of low doses of rapamycin (1-10nM) for 60 minutes.

(E) HeLa cells stably co-expressing sKin-Abl fragments (left gel) are activated only upon addition rapamycin (right gels). One hour treatment with 10 nM rapamycin induces sKin-Abl reassembly and corresponding kinase activation as measured by increased global phosphotyrosine as probed with either the pTyr-100 (middle) or pTyr-1000 antibody (right).

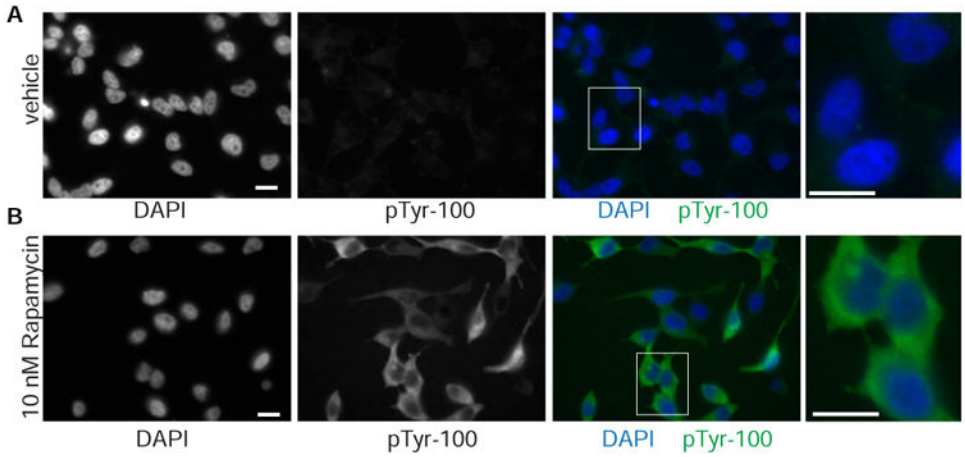

Figure 3. Activation of sKin-Abl lacking NLS leads to cytoplasmic pTyr and only in presence of rapamycin

(A) Immunofluorescent staining of pTyr in HeLa cells containing the sKin-Abl, which lacks the NLS of cAbl, in the absence of rapamycin. HeLa cells were treated with vehicle (0.01% DMSO) for 20 minutes and then stained with DAPI nuclear stain (blue) or pTyr-100 (green). Scale bar represents 20 μm.

(B) Parallel immunofluorescent staining as in **A**, with sKin-Abl activation following 20 minutes of incubation with 10 nM rapamycin shows phosphotyrosine is confined to the cytosol.

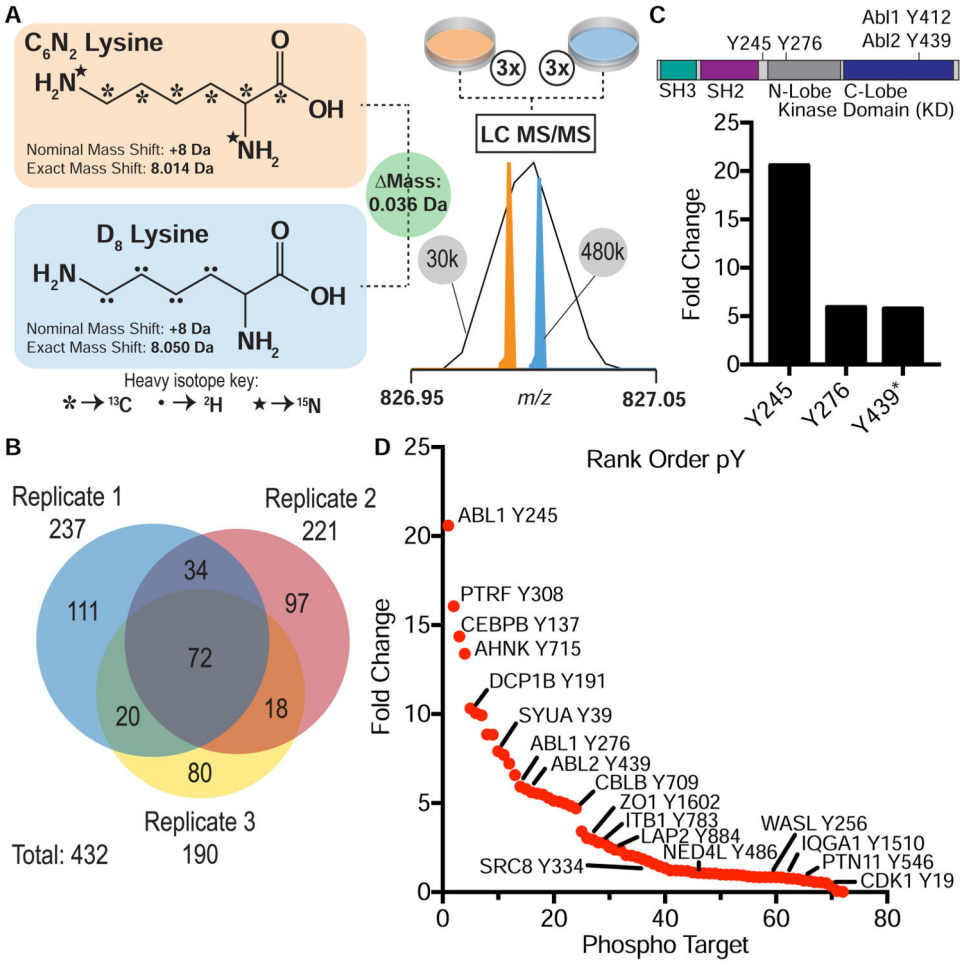

Figure 4. sKin-Abl Characterization of pTyr proteomics by Neucode SILAC

(A) Workflow for NeuCode SILAC experiments. Two heavy lysine isotopologues incorporate either ^{13}C and ^{15}N (orange) or ^{2}H (blue) to produce an equivalent nominal mass shift (+8 Da) but differing in exact masses (a total mass defect of 0.036 Da). This small mass difference is masked when medium resolving powers (*e.g.*, 30k) are employed, and only one peak appears in the spectrum employed (black trace in right panel). High resolution MS (*e.g.*, 480k), however, reveals the closely spaced NeuCode peaks (colored traces) to enable quantitation. In this experiment, sKin-ABL HeLa cells were cultured using either lysine isotopologue 602 (orange, +rapamycin) or 080 (blue, -rapamycin). Cells were treated either with or without rapamycin for 30 min, lysed, digested, mixed together, and processed together from fractionation through LC-MS/MS analysis.

(B) Venn diagram shows overlap between biological triplicate experiments using Neucode based SILAC labeling and quantitation. We observe a total of 432 pTyr sites of which 72 are in common across all three biological replicates and compose our filtered and high confidence dataset.

(C) Quantified pTyr isoforms that were identified in Neucode labeling and quantification. ABL1: Y245, SH2 kinase linker: necessary for full kinase activation, Y276, kinase domain/N-lobe, ABL2: Y439 corresponds to ABL1 Y412 -activation loop. All three pTyr sites were labeled only by activation of sKin-Abl and have high confidence values ($P<0.01$).

(D) Coverage and rank order of 72 common pTyr sites according to the observed fold change upon sKin-Abl activation. The labeled pTyr proteins either have been previously observed in the literature or highly annotated biological targets of interest. See Table S2 for complete list of all replicates and quantitation, including pT and pS events.

Key Resources Table

REAGENT or RESOURCE	SOURCE	IDENTIFIER
Antibodies		
Anti-FLAG M2 and Anti FLAG HRP Conjugate	Sigma	#F1804 & #A8592
Anti Src	Thermo-Scientific	MA5-15120
Anti-Phospho-Src Y416	Cell Signaling Technology	#2113
Anti-Phospho-Abl Y412	Cell Signaling Technology	#2865
Phospho-Y-100 & Phospho-Y-1000	Cell Signaling Technology	#9411 & #8954
Anti-GAPDH	Cell Signaling Technology	#14C10
Anti-Myc Tag (mouse & rabbit)	Cell Signaling Technology	#2276 & #71D10
Anti-Phospho-AktT308 & S473	Cell Signaling Technology	#13038 & #4060
Anti-p70 S6 Kinase & phopspho-p70 S6K (T389)	Cell Signaling Technology	#9202 & #9234
Goat anti-Mouse-HRP	Thermo Scientific	#31430
Goat anti-Rabbit-HRP	Thermo Scientific	#31460
Alexa Fluor 488 anti-mouse #A11029	Life Technologies	#A11029
Alexa Fluor 647 anti-rabbit	Life Technologies	#A21245
Bacterial and Virus Strains		
DH5 alpha, subcloning efficiency	Life Technologies	#18265017
Biological Samples		
Chemicals, Peptides, and Recombinant Proteins		
Rapamycin	Cayman Chemicals	#53123-88-9
Imatnib	Selleckchem	#S2475
NeuCode labeling reagents: L-Lysine:2HCl (3,3,4,4,5,5,6,6-D8, 98%)) and L-Lysine:2HCl (13C6, 99%, 15N2, 99%)	Cambridge Isotopes	#DLM-2641-0 & #CNLM-291-H-0.25
Critical Commercial Assays		
Deposited Data		
Experimental Models: Cell Lines		
Human: HEK293 Cells	UCSF Cell Core	
Human: HeLa Cells	UCSF Cell Core	
Experimental Models: Organisms/Strains		
Oligonucleotides		
Primers & gBlocks Gene Fragments	IDT	
Recombinant DNA		
pQCXI P/H	Clontech	631515
pcDNA3.1	Invitrogen	V790-20
Software and Algorithms		
Prism 6	Graphpad	
Excel	Microscoft	Office 2016 for Mac
Proteome Discoverer	Thermo Fisher	
NeuQuant, Opensource Software	Baughman et al. 2016	

REAGENT or RESOURCE	SOURCE	IDENTIFIER
PhosphoRS/COMPASS	Taus et al. 2011	
Other		
Lipofectamine 2000	Life Technologies	11668019